JOURNAL OF AGRICULTURAL AND FOOD CHEMISTRY

Article

pubs.acs.org/JAFC

Conjugation of the Mycotoxins Alternariol and Alternariol Monomethyl Ether in Tobacco Suspension Cells

Andreas A. Hildebrand, Beate N. Kohn, Erika Pfeiffer, Daniel Wefers, Manfred Metzler, and Mirko Bunzel*

Institute of Applied Biosciences, Department of Food Chemistry and Phytochemistry, Karlsruhe Institute of Technology (KIT), Adenauerring 20a, 76131 Karlsruhe, Germany

Supporting Information

ABSTRACT: The mycotoxins alternariol (AOH) and alternariol-9-*O*-methyl ether (AME) carry three and two phenolic hydroxyl groups, respectively, which makes them candidates for the formation of conjugated metabolites in plants. Such conjugates may escape routine methods of analysis and have therefore been termed masked or, more recently, modified mycotoxins. We report now that AOH and AME are extensively conjugated in suspension cultures of tobacco BY-2 cells. Five conjugates of AOH were identified by MS and NMR spectroscopy as β-D-glucopyranosides (attached in AOH 3- or 9-position) as well as their 6′-malonyl derivatives, and as a gentiobiose conjugate. For AME, conjugation resulted in the D-glucopyranoside (mostly attached in the AME 3-position) and its 6′- and 4′-malonyl derivatives. Pronounced differences were noted for the quantitative pattern of AOH and AME conjugates as well as for their phytotoxicity. Our *in vitro* study demonstrates for the first time that masked mycotoxins of AOH and AME can be formed in plant cells.

KEYWORDS: *masked mycotoxins, modified mycotoxins, Alternaria toxins, malonyl glucosides, plant cell culture*

INTRODUCTION

The cosmopolitan genus *Alternaria* contains many species that are important plant pathogens, infesting all the aerial parts of plants and causing, e.g., early blight diseases of vegetables, brown spot of tangerines, or postharvest black rot of fruit.[1] In addition to economic losses due to preharvest and postharvest decay, *Alternaria* species produce several groups of toxins, which contaminate food and feed and may pose a health problem.[2] For example, *Alternaria* toxins have been associated with an increased incidence of esophageal cancer in certain areas of China.[3] In 2011, the European Food Safety Authority (EFSA) published a Scientific Opinion on the risks for animal and public health related to the presence of *Alternaria* toxins in feed and food.[4] The analysis of 11 730 occurrence data showed that the most frequently detected *Alternaria* toxins were the dibenzo-α-pyrones alternariol (AOH) and alternariol-9-*O*-monomethyl ether (AME) (Figure 1A,B), which were common contaminants of cereals, sunflower seeds, oilseed rape, olives, various fruits, and other food items.[4] AOH and AME exhibit genotoxicity *in vitro* by inducing gene mutations, DNA strand breaks, and inhibition of topoisomerase I and IIα.[5−8]

Both AOH and AME have free hydroxyl groups available for metabolic conjugation (Figure 1A,B). In the mammalian organism, formation of glucuronides is a major pathway of detoxification and excretion. *In vitro* studies have shown that AOH and AME are readily converted to glucuronides upon incubation with hepatic and intestinal microsomes from humans, rats, and pigs in the presence of UDPGA.[9] Whereas AOH gave rise to comparable amounts of the 3-*O*-glucuronide and 9-*O*-glucuronide, AME was predominantly converted to the 3-*O*-glucuronide. In the same study, the activities of 10 recombinant human UDP-glucuronosyltransferases for AOH and AME were determined; nine were found to be active for AOH and eight for AME.

Over the past years, researchers and regulators have become aware that conjugation of mycotoxins (and other compounds such as pesticides) may also occur in plants. Such conjugation reactions are believed to be part of the detoxification system of the plant.[10] Xenobiotic and endogenous compounds carrying hydroxyl groups are frequently converted to glucosides and further processed by addition of a malonyl, hexose, or pentose moiety to facilitate compartmentation and storage.[10] Conjugated compounds escape routine methods of analysis if the method aims exclusively at the detection of the parental compounds. However, upon ingestion of the conjugate by humans or animals, the parental form may be released in the digestive tract and absorbed, thereby increasing the total exposure to the compound. For the first time, this has been unambiguously demonstrated for a glucoside of the mycotoxin zearalenone, and the term "masked mycotoxin" has been coined.[11] Today, several masked forms of zearalenone and other mycotoxins, in particular of trichothecenes like deoxynivalenol and nivalenol are known.[12,13] More recently, the term "modified mycotoxins" has been proposed for a comprehensive definition including, e.g., derivatives formed by thermal reactions or by plant metabolism (so-called "masked" mycotoxins).[14]

Because it is yet unknown whether AOH and AME are converted to conjugated metabolites in plants, the aim of this

Received: February 11, 2015
Revised: April 23, 2015
Accepted: April 25, 2015
Published: April 25, 2015

DOI: 10.1021/acs.jafc.5b00806
J. Agric. Food Chem. 2015, 63, 4728−4736

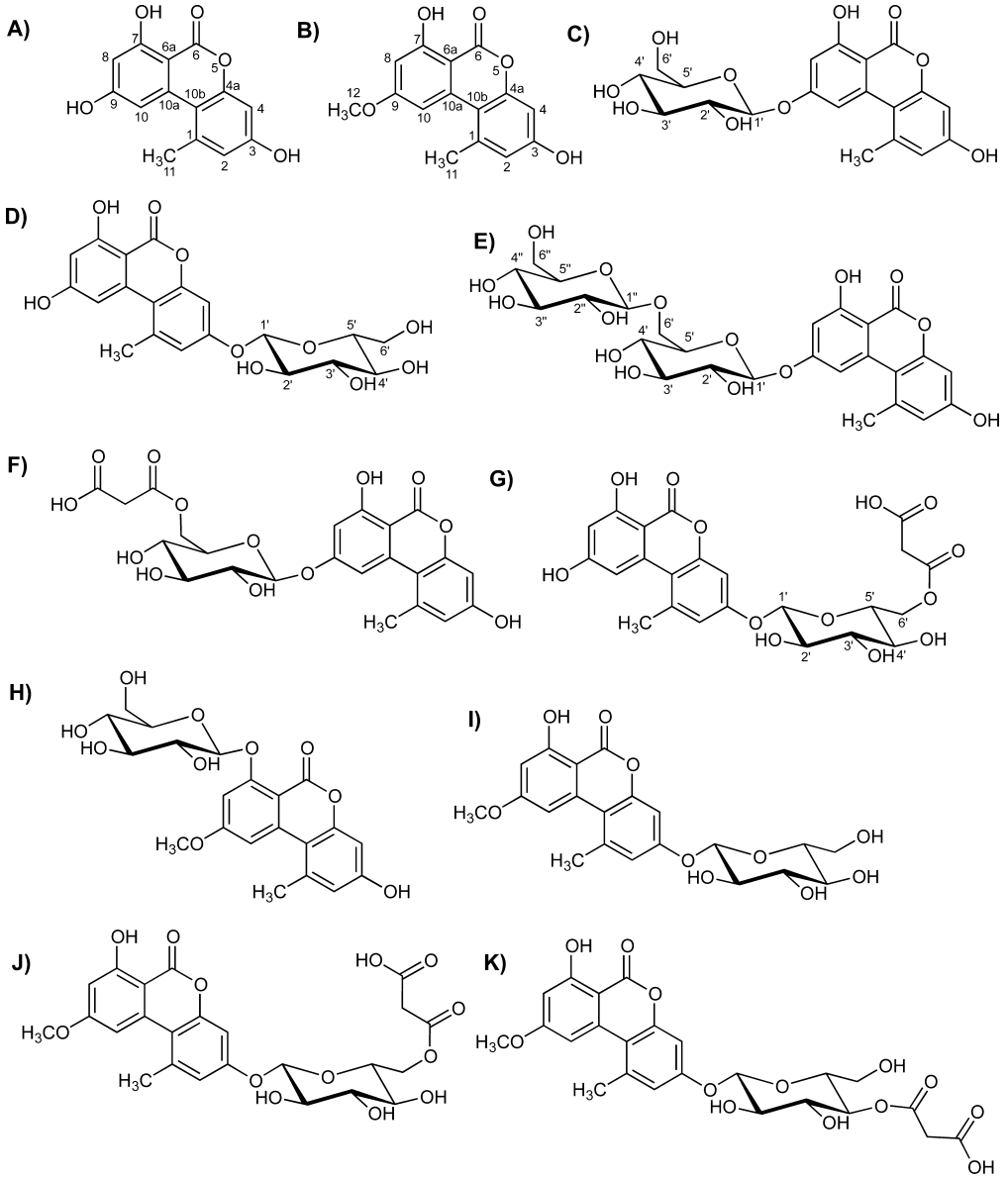

Figure 1. Chemical structures of alternariol (AOH, A), alternariol-9-*O*-monomethyl ether (AME, B), and AOH and AME metabolites formed in a tobacco suspension cell culture system. 9-*O*-*β*-D-glucopyranosyl-AOH (AOH-2, C); 3-*O*-*β*-D-glucopyranosyl-AOH (AOH-3, D); 9-*O*-{*β*-D-glucopyranosyl(1 → 6)-*β*-D-glucopyranosyl}AOH (AOH-1, E); 9-*O*-(6-*O*-malonyl-*β*-D-glucopyranosyl)AOH (AOH-4, F); 3-*O*-(6-*O*-malonyl-*β*-D-glucopyranosyl)AOH (AOH-5, G); 7-*O*-*β*-D-glucopyranosyl-AME (AME-2, H); 3-*O*-*β*-D-glucopyranosyl-AME (AME-5, I); 3-*O*-(6-*O*-malonyl-*β*-D-glucopyranosyl)AME (AME-6, J); 3-*O*-(4-*O*-malonyl-*β*-D-glucopyranosyl)AME (AME-7, K).

study was to analyze AOH and AME conjugation in a tobacco BY-2 suspension cell culture as a model system.

MATERIALS AND METHODS

Chemicals and Reagents. AOH and AME were isolated from a culture of *Alternaria alternata* strain TA7 grown on rice flour containing media for 24 days at 25 °C as described earlier for the isolation of other *Alternaria* toxins.[15] The crude extract was analyzed by LC-MS, and the fractions containing AOH and AME were isolated by preparative HPLC. Identity was confirmed by NMR (see below), and the purity was >98% according to HPLC analysis with UV detection at 254 nm.

Chemicals for the tobacco cell culture and other chemicals and reagents were obtained from Sigma-Aldrich/Fluka (Taufenkirchen, Germany) and Duchefa (Haarlem, The Netherlands) and were of the highest quality available (96−100% depending on the chemical, with the exception of Evan's Blue (>75% purity)). HPLC-MS grade acetonitrile and methanol were purchased from VWR International (Bruchsal, Germany). NMR solvents were from Deutero GmbH (Kastellaun, Germany) and VWR International.

Tobacco Suspension Cell Culture. Tobacco BY-2 cells (*Nicotiana tabacum* L. cv. Bright Yellow 2) were kindly provided by Dr. Jan Maisch (Institute of Botany, KIT). The cells were cultured in the dark at 25 °C on an orbital shaker at 150 rpm in 100 mL Erlenmeyer flasks containing 30 mL of Murashige and Skoog medium supplemented with 30 g/L sucrose, 200 mg/L KH_2PO_4, 100 mg/L inositol, 1 mg/L thiamine, and 0.2 mg/L 2,4-dichlorophenoxyacetic acid. The medium was adjusted to pH 5.8. The cells were subcultured weekly, transferring 1.5 mL (about 0.5 g cell wet weight) of the suspension into 30 mL of fresh medium. The exponential growth phase of the cells started after 3 days and was finished on day seven (about 10 g of cell wet weight or 0.4−0.5 g of cell dry weight in the stationary phase).

Incubation of Tobacco Cells with AOH and AME. Stock solutions (10 mM) of AOH or AME in DMSO were stable at ambient

DOI: 10.1021/acs.jafc.5b00806
J. Agric. Food Chem. 2015, 63, 4728−4736

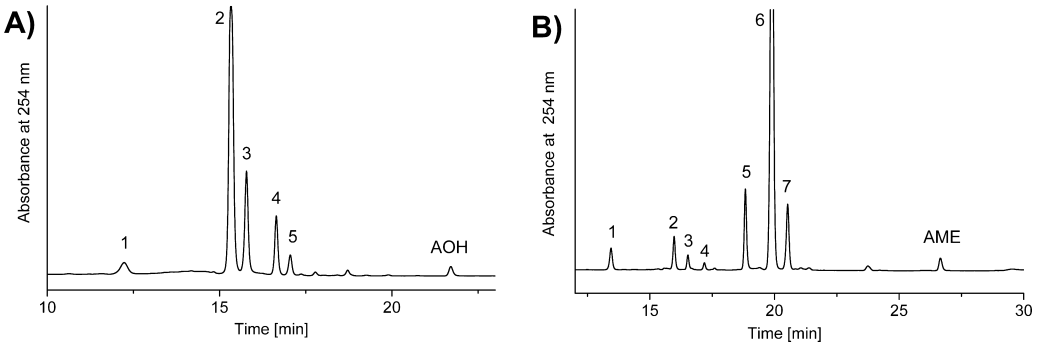

Figure 2. HPLC profiles of metabolites of alternariol (AOH) (A) and alternariol-9-*O*-monomethyl ether (AME) (B) in extracts of cultured tobacco BY-2 cells after 48 h incubation (UV detection at 254 nm). The abbreviations used for the metabolites (AOH-X, AME-X) indicate which metabolite is represented by which peak in the chromatogram (with X describing the peak number).

temperature in the dark for up to two months. The concentration of the mycotoxin in the incubation medium was 50 or 100 μM. The DMSO concentration did not exceed 1%. Control incubations were carried out with DMSO but without mycotoxin. After 24, 48, or 96 h of incubation, cells and medium were separated by filtration and freeze-dried. The dried medium was dissolved in MeOH for chromatographic analysis. The dried cells (10−12 g wet cells yield about 0.6 g dry cells) were ground using mortar and pestle. To extract AOH, AME, and their metabolites, an optimized extraction procedure was used: 0.1 g of the ground material was extracted twice for 2 h at 25 °C with horizontal shaking. For the first extraction, 4.5 mL of MeOH/CH_2Cl_2 (2:1, v/v) was used, whereas 4.5 mL of MeOH/H_2O/acetic acid (79/20/1, v/v/v) was used for the second extraction. The combined extracts were evaporated to dryness using a vacuum evaporator, and the residues were dissolved in 0.4 mL of MeOH and analyzed by using HPLC-photo diode array (PDA)-MS.

Assay To Determine Cell Death. Cells that accumulated Evans blue were considered as dead cells.[16] An aliquot of the cell suspension (200 μL) was incubated with 1.5 mL of 0.05% (w/v) Evans blue at room temperature for 15 min, subsequently washed twice with 1 mL of PBS, and resuspended in 500 μL of PBS. An aliquot of the suspension (20 μL) was transferred on microscope slides, and a total of 500 cells was scored under the light microscope, discriminating between living (uncolored) and dead (blue stained) cells.

HPLC-PDA-MS Analysis. An LXQ Linear Ion Trap MS^n system (Thermo Fisher Scientific, Waltham, MA, USA) equipped with a Finnigan Surveyor HPLC-PDA system was used. Separation was carried out on a reversed phase column (Phenomenex Luna C8(2), 250 × 4.6 mm i.d.). Solvent A was H_2O with 0.1% formic acid, solvent B was acetonitrile with 0.1% formic acid, and the flow rate was 0.5 mL/min. The linear gradient started with 20% B, held for 5 min, ramped to 50% B in 10 min, ramped to 70% B in 9 min, ramped to 100% B in 5 min, held for 2 min, decreased to 20% B in 1 min, and equilibrated for 2 min before the next injection. The metabolites were detected at 254 nm and characterized with MS operating in ESI positive mode. Full scan mass spectra were recorded from m/z 100−1000, MS^2 of the $[M + H]^+$ ions was conducted at CID 35 (35% of 5 V). Nitrogen was used as the sheath gas, auxiliary gas, and sweep gas with flow rates of 30.0, 15.0, and 0.02 L/min, respectively. Spray voltage was 4.47 kV, spray current 3.15 mA, capillary voltage 45.10 V, capillary temperature 350 °C, and the tube lens voltage was 125.58 V. Semiquantitative analyses were carried out by determining peak areas at 254 nm, using AOH or AME as external standard compounds.

Isolation of the Metabolites of AOH and AME. About 12 g of dry cells were collected from several incubations of each mycotoxin and extracted by scaling up the procedure described above, yielding about 40 mL of crude extracts dissolved in MeOH. These extracts were fractionated in portions of 1.5 mL using a preparative HPLC-UVD system (LC-8A pumps, SPD-20A UV detector, Shimadzu, Kyoto, Japan) and a reversed phase column (Phenomenex, Luna C18(2), 5 μm, 250 × 25.0 mm i.d.). Solvent A was water with 0.1% formic acid, solvent B was MeOH with 0.1% formic acid, and the flow rate was 8 mL/min. A linear gradient was started with 20% B held for 5 min, then ramped to 65% B in 20 min, ramped to 90% B in 1 min, and held for 4 min. Fractions of the separated metabolites were collected manually according to the chromatograms. After vacuum-concentration to about half of their volumes, the fractions were freeze-dried for HPLC-PDA-MS and NMR analysis. HPLC-PDA-MS was conducted as described above and showed that the purity of the AOH and AME metabolites used for NMR analysis was >97% (based on UV chromatograms at 254 nm).

Carbohydrate Analysis. Carbohydrate analysis was performed by high performance anion exchange chromatography (HPAEC) with pulsed amperometric detection (PAD) after acidic hydrolysis with 2 M trifluoroacetic acid for 30 min at 121 °C. After evaporation of the acid, the sample was redissolved in water and analyzed on an ICS-5000 HPAEC system (Thermo Scientific Dionex, Sunnyvale, CA, USA) using a CarboPac PA-20 column. The exact chromatographic conditions are described in Wefers et al. (2014).[17] To determine D-/L-configuration of the glucose unit in 9-*O*-β-glucopyranosyl-AOH, the glycosidic linkage was cleaved as described above. The residue after evaporation was derivatized with 150 μL of (*R*)-2-octanol and 5 μL of TFA at 130 °C overnight. After removal of the derivatization reagents, the sample was silylated by using 80 μL of *N*,*O*-bis(trimethylsilyl) trifluoroacetamide and 20 μL of pyridine. Sample analysis was performed by GC-MS (GC-2010 Plus and GCMS-QP2010 Ultra, Shimadzu, Kyoto, Japan) equipped with an Rxi-5Sil MS column (30 m × 0.25 mm i.d., 0.25 μm film thickness, Restek, Bad Homburg, Germany). Detailed chromatographic conditions are given in Wefers et al. (2014).[17]

NMR Spectroscopy. NMR spectra were recorded on a Bruker Ascend^M 500 spectrometer (Rheinstetten, Germany) equipped with a Prodigy cryoprobe. Freeze-dried samples were dissolved in 500 μL of DMSO-d_6. The structures of the isolated oligosaccharides were identified by using ^{1}H, H,H-correlated spectroscopy (COSY), heteronuclear single quantum coherence (HSQC), and heteronuclear multiple bond correlation (HMBC) experiments. Standard Bruker pulse sequences were used; spectra were acquired at 298 K. Chemical shifts (δ) were referenced to the central solvent signals (δH 2.50 ppm and δC 39.5 ppm).[18]

RESULTS AND DISCUSSION

Metabolite Patterns of AOH and AME Obtained from Tobacco BY-2 Cells. AOH and AME were incubated in tobacco BY-2 cell suspensions for 2 days during the exponential growth phase. The incubation medium after cell separation did not contain detectable amounts of free AOH and AME, suggesting complete mycotoxin uptake into the cells. Analysis of the cell extracts after disruption of the intact cells revealed the presence of small amounts of parental AOH and AME. The major part of the mycotoxins was, however, metabolized as demonstrated by five and seven peaks with spectroscopic

DOI: 10.1021/acs.jafc.5b00806
J. Agric. Food Chem. 2015, 63, 4728−4736

Table 1. ^{1}H and ^{13}C NMR Data of Alternariol (AOH) and Its Metabolites[a]

	AOH (Figure 1A)			AOH-1 (Figure 1E)			AOH-2 (Figure 1C)			AOH-3 (Figure 1D)			AOH-4 (Figure 1F)			AOH-5 (Figure 1G)		
	δ_H	J	δ_C	δ_H	J	δ_C	δ_H	J	δ_C	δ_H	J	δ_C	δ_H	J	δ_C	δ_H	J	δ_C
1			138.10			138.33			138.36			138.07			138.12			138.33
2	6.72	d (2.3)	117.32	6.74	d (2.3)	117.44	6.74	d (2.2)	117.50	6.96	d (2.4)	117.82	6.73	d (2.1)	117.30	6.94	d (2.6)	117.50
3			158.25			158.44			158.42			157.42			158.62			157.15
3-OH	10.35	s		10.66	s		10.46	s					10.44	s				
4	6.64	d (2.3)	101.36	6.67	d (2.3)	101.38	6.66	d (2.2)	101.28	6.97	d (2.4)	102.16	6–64	d (2.1)	101.31	6.97	d (2.6)	102.16
4a			152.51			152.37			152.55			152.27			152.70			153.80
6			163.99			nd			nd			nd			nd			nd
6a			97.21			99.29			99.42			97.25			99.75			98.09
7			164.44			163.75			163.49			163.90			164.11			164.33
7-OH	11.77	s					11.76	s		nd			11.78	s		11.74	s	
8	6.37	d (1.6)	100.63	6.75	d (1.8)	101.33	6.64	d (1.5)	101.45	6.41	d (1.3)	101.27	6.70	d (1.2)	101.41	6.42	d (1.7)	101.16
9			165.29			163.70			163.78			165.66			163.48			165.59
9-OH	10.92	s								nd						nd		
10	7.25	d (1.6)	104.07	7.37	d (1.8)	104.15	7.40	d (1.5)	103.97	7.30	d (1.3)	104.84	7.32	d (1.2)	103.95	7.32	d (1.7)	104.62
10a			138.10			138.33			138.36			138.07			138.12			138.33
10b			108.75			108.36			108.61			111.04			108.75			111.65
11	2.71	s	24.97	2.75		24.93	2.76	s	24.86	2.76	s	24.99	2.75	s	24.82	2.77	s	24.94
1′				5.14	d (7.2)	99.41	5.13	d (7.3)	99.62	5.02	d (7.4)	99.75	5.14	d (7.4)	99.46	5.08	d (7.4)	99.24
2′				3.29		72.80	3.29		72.85	3.25		72.93	3.31		72.74	3.29		72.75
3′				3.31		75.85	3.32		76.06	3.28		76.33	3.35		75.68	3.32		75.93
4′				3.24		69.18	3.17		69.39	3.16		69.40	3.18		69.49	3.20		69.33
5′				3.69		75.28	3.43		77.19	3.42		76.93	3.73		73.75	3.75		73.43
6′				3.97		68.38	3.72		60.45	3.70		60.42	4.40		63.80	4.37		63.83
6′				3.62		68.37	3.47		60.45	3.45		60.43	4.07		63.75	4.12		63.78
1′′				4.16	d (7.8)	103.37												
2′′				2.95		73.24												
3′′				3.05		76.66												
4′′				3.05		69.74												
5′′				3.10		76.44												
6′′				3.64		60.77												
6′′				3.42		60.74												
Mal-CH_2													3.24		42.19	3.39		41.20
Mal-*COOR*															167.37			nd
Mal-*COOH*													12.20		167.80	11.00		167.80

[a]AOH-1:9-*O*-{*β*-D-glucopyranosyl(1 → 6)-*β*-D-glucopyranosyl}AOH; AOH-2:9-*O*-*β*-D-glucopyranosyl-AOH; AOH-3:3-*O*-*β*-D-glucopyranosyl-AOH; AOH-4:9-*O*-(6-*O*-malonyl-*β*-D-glucopyranosyl)AOH; AOH-5:3-*O*-(6-*O*-malonyl-*β*-D-glucopyranosyl)AOH. δ_H/δ_c are given in ppm, J in Hz. nd = not determined, s = singlet, d = doublet

DOI:10.1021/acs.jafc.5b00806
J. Agric. Food Chem. 2015, 63, 4728−4736

characteristics suggesting AOH and AME conjugates, respectively (Figure 2). None of these peaks was present in control incubations without mycotoxins. Variation of the mycotoxin concentration, incubation time, and cell mass did not change the number of potential conjugates, although slight changes in the size of the peaks were observed. All potential conjugates eluted earlier than AOH or AME from the reversed-phase column and had characteristic UV spectra similar to that of the parental mycotoxins, i.e., with absorption bands at about 254, 288, 299, and 340 nm. The m/z values of the quasi-molecular ions of the potential conjugates were higher than those of the parental compounds, but their MS^2 spectra showed the m/z values of the corresponding mycotoxins as major fragments.

To obtain sufficient quantities of the metabolites for structure elucidation, the combined cell extracts of several incubations were fractionated using preparative HPLC. All five metabolites of AOH and four dominant AME metabolites represented by peaks 2, 5, 6, and 7 (Figure 2) were isolated in quantities and purities that allowed for unambiguous structural characterization by NMR spectroscopy. The minor AME metabolites 1, 3, and 4 were isolated in small amounts only. Tentative structures could, however, be proposed based on their UV and mass spectrometric data as discussed later.

Structure Elucidation of the Major AOH and AME Conjugates. *AOH Metabolites.* The molecular mass of the AOH metabolite representing the dominant peak 2 (Figure 2A) was determined as 420 (quasi-molecular ion with m/z 421 $[M + H]^+$) consistent with a metabolite built of AOH and a hexose sugar. The mass difference between the quasi-molecular ion and the fragment m/z 259 $[AOH + H]^+$ also suggests AOH being attached to a hexose. HPAEC-PAD analysis after acidic hydrolysis revealed the hexose to be glucose. The aromatic region of the ^1H NMR spectrum of AOH metabolite 2 showed four AOH doublets with 2 Hz *meta* coupling constants. The carbons shifts of AOH were assigned by using the HSQC and HMBC spectra. Comparison of the ^1H and ^{13}C chemical shifts (Table 1) with those of parental AOH showed larger differences for C9, H8, and H10 suggesting a modification at the phenolic hydroxyl group attached to C9. Because DMSO was used as a solvent, intermolecular proton exchanges were slowed down resulting in several discrete OH signals in most samples. By using the HMBC experiment the phenolic OH protons can be assigned to specific carbons. Here, HMBC correlation peaks showed coupling of the phenolic proton in position 7, demonstrating that this phenolic group was not conjugated. The anomeric proton signal of the glucose moiety showed a coupling constant of 7.3 Hz implicating the β-anomer of the glucose unit. The appearance of one anomeric proton only and comparison of the ^1H and ^{13}C NMR data with those of glucose suggested the glucose to be bound via its lactol group to AOH. An HMBC correlation peak (Figure 3A) between the anomeric proton and C9 of AOH confirmed the glycosidic linkage in the suggested position and proved this compound to be 9-*O*-β-D-glucopyranosyl-AOH (Figure 1C).

Structure elucidation of the compound representing peak 3 (Figure 2A) showed many similarities to 9-*O*-β-D-glucopyranosyl-AOH. However, NMR data clearly demonstrate the linkage between the β-anomer of the glucose unit and the phenolic hydroxyl group in position C3 of AOH via a glycosidic linkage, identifying this compound as 3-*O*-β-D-glucopyranosyl-AOH (Figure 1D).

The remaining three potential AOH conjugates had molecular masses different from AOH glucosides. The mass

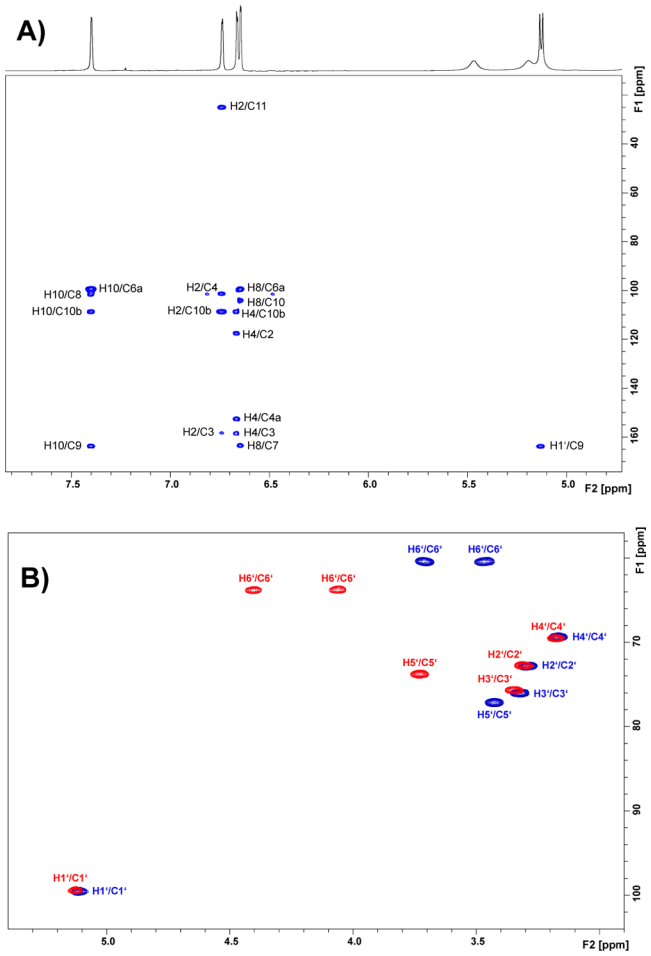

Figure 3. (A) HMBC spectrum (aglycone and anomeric region) of 9-*O*-β-D-glucopyranosyl-alternariol. (B) Overlay of the carbohydrate regions of the HSQC spectra of 9-*O*-β-D-glucopyranosyl-alternariol (blue correlation peaks) and 9-*O*-(6-*O*-malonyl-β-D-glucopyranosyl)-alternariol (red correlation peaks).

spectrum of peak 1 showed quasi-molecular ions with m/z 583 ($[M + H]^+$) and m/z 605 ($[M + Na]^+$), indicating a molecular mass of 582. Two mass losses of 162 Da resulting in m/z 421 and m/z 259 suggested that AOH is attached to a hexose disaccharide. NMR data confirmed this assumption and demonstrated an (1 → 6)-linkage between the two glucopyranose units (diagnostic HMBC signals, downfield shift of about 8 ppm for C6 of one glucose unit). Again, the coupling constants of the anomeric protons (7.2 Hz, 7.8 Hz) demonstrated both glucose anomers to be in their β-position. NMR data of the aglycone suggested its conjugation via the phenolic OH group at C9, which was unambiguously verified by interpretation of the HMBC spectrum. Thus, the compound representing peak 1 was identified as 9-*O*-{β-D-glucopyranosyl-(1 → 6)-β-D-glucopyranosyl}AOH (Figure 1E).

The quasi-molecular ions of the compounds representing peaks 4 and 5 (m/z 507, $[M + H]^+$; m/z 529, $[M + Na]^+$) suggest a molecular mass of 506 that cannot be explained by the formation of simple AOH glycosides. The MS^2 spectra showed a 248 Da mass loss resulting in a fragment with m/z 259 $[AOH + H]^+$. A mass loss of 248 Da indicates the elimination of an anhydro malonylglucoside as was also observed for isoflavone malonylglucosides.[19] Interpretation of the NMR spectra confirmed the substitution of the glucose unit

DOI: 10.1021/acs.jafc.5b00806
J. Agric. Food Chem. 2015, 63, 4728−4736

Table 2. ^{1}H and ^{13}C NMR Data of Alternariol-9-*O*-monomethyl Ether (AME) and Its Metabolites[a]

	AME (Figure 1B)			AME-2 (Figure 1H)			AME-5 (Figure 1I)			AME-6 (Figure 1J)			AME-7 (Figure 1K)		
	δ_H	*J*	δ_C	δ_H	*J*	δ_C	δ_H	*J*	δ_C	δ_H	*J*	δ_C	δ_H	*J*	δ_C
1			138.30			137.75			138.22			138.08			138.48
2	6.73	d (2.3)	117.42	6.68	d (2.4)	116.70	6.98	d (2.4)	117.94	6.96	d (1.8)	117.71	7.01	d (2.5)	117.95
3			158.33			158.30			157.60			157.18			157.65
3-OH	10.39	s		10.33	s										
4	6.65	d (2.3)	101.29	6.56	d (2.4)	100.72	6.99	d (2.4)	102.21	6.98	d (1.8)	102.28	7.03	d (2.5)	102.21
4a			152.52			152.67			152.22			152.11			152.19
6			nd			nd			nd			nd			nd
6a			98.47			nd			98.62			98.54			99.02
7			164.00			161.30			164.04			163.94			164.16
7-OH	11.83	s					11.78			11.80			11.81		
8	6.63	d (1.9)	98.94	6.97	d (2.1)	101.33	6.69	d (1.9)	99.56	6.68	d (1.1)	99.54	6.71	d (2.1)	99.60
9			165.89			164.17			165.92			165.71			166.07
10	7.23	d (1.9)	103.23	7.37	d (2.1)	104.21	7.30	d (1.9)	103.88	7.3	d (1.1)	103.89	7.32	d (2.1)	103.94
10a			138.30			137.75			138.22			138.08			138.48
10b			108.60			108.70			110.79			110.79			111.33
11	2.74	s	24.81	2.75		24.70	2.80		24.77	2.80		24.78	2.81		24.80
12	3.91	s	55.60	3.93		55.44	3.93		55.69	3.93		41.23	3.93		55.72
1′				5.01	d (7.7)	101.68	5.03	d (7.4)	99.74	5.1	d (7.3)	99.29	5.17	d (7.8)	99.31
2′				3.39		73.14	3.26		72.91	3.29		72.78	3.37		72.84
3′				3.31		76.04	3.28		76.30	3.32		76.03	3.76		74.04
4′				3.16		69.64	3.16		69.39	3.20		69.37	4.68		71.43
5′				3.43		77.33	3.44		76.92	3.75		73.46	3.55		73.46
6′				3.73		60.60	3.71		60.39	4.37		63.87	3.57		59.79
6′				3.45		60.60	3.45		60.38	4.12		63.87	3.35		59.74
Mal-CH_2										3.39		41.23	3.42		41.47
Mal-*COOR*												166.68			166.34
Mal-*COOH*										nd		167.30			168.22

[a]AME-2:7-*O*-*β*-D-glucopyranosyl-AME; AME-5:3-*O*-*β*-D-glucopyranosyl-AME; AME-6:3-*O*-(6-*O*-malonyl-*β*-D-glucopyranosyl)AME; AME-7:3-*O*-(4-*O*-malonyl-*β*-D-glucopyranosyl)AME. δ_H/δ_c are given in ppm, J in Hz. nd = not determined, s = singlet, d = doublet.

with a malonyl group. Linkage of the malonyl group to the glucose 6 position was obvious from the ^{1}H and ^{13}C data if compared to data of the non-malonyl conjugated AOH glucoside (Figure 3B, Table 1) and was confirmed by HMBC correlation peaks showing coupling of the malonyl carbonyl carbon and glucose 6 protons. Again, the glucose unit was proven to be in its *β*-configuration. NMR also revealed that the compounds representing peaks 4 and 5 differ in the AOH position to which the 6-*O*-malonyl-*β*-D-glucopyranosyl unit is attached. HMBC correlation peaks show the attachment to AOH position 9 (compound representing peak 4) and 3 (compound representing peak 5) identifying these AOH metabolites as 9-*O*-(6-*O*-malonyl-*β*-D-glucopyranosyl)AOH and 3-*O*-(6-*O*-malonyl-*β*-D-glucopyranosyl)AOH, respectively (Figure 1F,G).

AME Metabolites. Different from AOH, AME carries two phenolic hydroxyl groups only. Because of the methoxyl group in position 9, glycosidation in this position as shown for AOH is not an option. The quasi-molecular ion of peak 2 (Figure 2B) (*m*/*z* 457, $[M + Na]^+$) and the fragment *m*/*z* 273 ($[AME + H]^+$, mass loss of 162 Da) suggested AME to be conjugated with a hexose. NMR data (Table 2) indicated glucose conjugation of AME in position 7, which was confirmed by an HMBC correlation peak between the anomeric proton (*β*-configuration) and carbon 7 of AME identifying this compound as 7-*O*-*β*-D-glucopyranosyl-AME (Figure 1H).

The compound representing peak 5 has a molecular weight of 434 (quasi-molecular ion *m*/*z* 435, $[M + H]^+$), and its NMR-data are closely comparable to those of 3-*O*-*β*-D-glucopyranosyl-AOH with the exception of those data showing the difference between AOH and AME. Complete interpretation of the data including the HMBC correlation peak between the anomeric glucose proton and the AME C3 identified this compound as 3-*O*-*β*-D-glucopyranosyl-AME (Figure 1I).

The mass spectrum of the compound representing peak 6 suggested a malonyl conjugated AME glucoside (quasi-molecular ions of *m*/*z* 521 $[M + H]^+$ and *m*/*z* 543 $[M + Na]^+$, MS^2: *m*/*z* 273 $[AME + H]^+$). Independent interpretation of the NMR data but also comparison to the data of 3-*O*-(6-*O*-malonyl-*β*-D-glucopyranosyl)AOH suggested this compound to be 3-*O*-(6-*O*-malonyl-*β*-D-glucopyranosyl)AME. The linkage positions between AME, glucose, and the malonyl group were unambiguously confirmed by HMBC signals, identifying this compound as 3-*O*-(6-*O*-malonyl-*β*-D-glucopyranosyl)AME (Figure 1J).

Another malonyl glucoside of AME was obtained from peak 7. Again, both the quasi-molecular of *m*/*z* 521 ($[M + H]^+$) and the loss of 248 Da (representing an anhydro malonylglycoside) were indicative for such a structure. NMR data of the AME moiety of this compound were closely comparable to those of 3-*O*-(6-*O*-malonyl-*β*-D-glucopyranosyl)AME; however, large differences were found for the NMR data of the glucose moiety. A downfield shift of the glucose C4 signal and upfield shifts of both the C3 and C5 signals indicate the attachment of the malonyl group to the glucose 4 position, which was also confirmed by interpretation of the HMBC spectrum. Using the described information, this compound was identified as 3-*O*-(4-*O*-malonyl-*β*-D-glucopyranosyl)AME (Figure 1K).

Thus, all metabolites of AOH and AME contain *β*-glucopyranose linked through a glycosidic bond to various

DOI: 10.1021/acs.jafc.5b00806
J. Agric. Food Chem. 2015, 63, 4728−4736

hydroxyl groups of the mycotoxins. To prove that glucose was in its D-configuration, 9-*O*-*β*-D-glucopyranosyl-AOH was hydrolyzed under acidic conditions. The liberated glucose was derivatized with (*R*)-2-octanol, silylated, and analyzed by GC-MS confirming that glucose was present in its D-form. From these results it was assumed that all glucose units in the identified AOH and AME conjugates were in their D-configuration. Whereas both available phenolic hydroxyl groups (in 3- and 7-position) of AME were found conjugated with glucose, a conjugate in which the phenolic hydroxyl group in position 7 of AOH was substituted with glucose was not found as a major AOH conjugate. Lack of conjugation may be due to the hydroxyl group being engaged in hydrogen bonding with the neighboring carbonyl group at C6 (Figure 1). In contrast, 7-*O*-glucosylation occurred in the conjugation of AME to a small extent; 3-*O*-glucosylation was, however, predominant (see below). A similar difference in the conjugation of AOH and AME was observed in an *in vitro* study on the glucuronidation with human hepatic microsomes and recombinant human UDP-glucuronosyl transferases (UGTs). AOH was glucuronidated at the C3 and C9, but not C7 hydroxyl groups, and the rate and ratio of C3 and C9 conjugation were dependent on the individual UGT isoform.[9] For AME, glucuronidation was clearly preferred at C3 by most UGT isoforms, but a few isoforms, e.g., UGT1A7, catalyzed the conjugation at C7. Similar differences in the conjugation can be assumed for plant cells, which are known to differ in their pattern of UDP-glucosyltranferases.[12] For example, Kovalsky Paris et al. (2014) recently identified an UDP-glucosyltransferase from barley, which did not catalyze the common glucosylation of zearalenone at the 14-hydroxyl group only, which is equivalent to the 9-hydroxyl of AOH, but also at the 16-hydroxyl group, which is neighboring a carbonyl group similar to the 7-hydroxyl groups of AOH and AME.[20]

The monoglucosides are, in part, further conjugated at the glucopyranoside moiety with another *β*-D-glucopyranose (forming a gentiobiose conjugate). A gentiobiose conjugate was unambiguously identified for AOH only. However, the MS spectra and HPLC retention times of AME peaks 1 and 3 (Figure 2B) also suggest the existence of an AME-7-diglucoside and an AME-3-diglucoside, respectively. Because NMR spectra were not obtained from the minor quantities of these metabolites, the position of conjugation was deduced from the observation that metabolites with identical conjugate moiety are eluted earlier if conjugated at C7 as compared to those conjugated at C3. In addition, two malonyl glucosides of AOH and two malonyl glucosides of AME were unambiguously identified. On the basis of its mass spectrum and elution behavior a fifth malonyl glucoside was tentatively identified as 7-*O*-(6-*O*-malonyl-*β*-D-glucopyranosyl)AME. Earlier studies describe a malonyl migration for malonyl glucosides of various phytochemicals such as isoflavones. Acyl migration, especially 4 → 6 migrations, are frequently described in the literature.[21] Exemplarily, 4 → 6 migration was observed for malonylgenistin.[19] Therefore, solutions of the isolated AME malonyl glucosides in MeOH and DMSO were tested for their stability. Both compounds 3-*O*-(6-*O*-malonyl-*β*-D-glucopyranosyl)AME and 3-*O*-(4-*O*-malonyl-*β*-D-glucopyranosyl)AME were stable within the test period of up to 2 weeks.

Quantitative Aspects of AOH and AME Conjugation in Tobacco BY-2 Cells. Although it was not the aim of this study to exactly quantitate the metabolites and investigate the kinetics of their formation, a striking difference in the quantitative pattern of the metabolites of AOH and AME was noted. After 48 h incubation of AME (50 μM in medium), about 75% of the applied amount was recovered in the form of extractable conjugates. Conjugation with glucose took place at the phenolic hydroxyl groups located at positions C3 (about 90%) and C7 (10%) (Figure 2B). About 10% of the recovered metabolites remained as the monoglucoside 3-*O*-*β*-D-glucopyranosyl-AME, whereas 80% were further metabolized by malonylation, preferentially (70%) at the glucose 6 position but also at the 4 position (10%). The only notable change in the pattern of AME metabolites due to varying incubation times concerned the proportion of 3-*O*-*β*-D-glucopyranosyl-AME, which decreased from 25% after 24 h incubation to 5% after 96 h, with a concomitant increase of 3-*O*-(6-*O*-malonyl-*β*-D-glucopyranosyl)AME (data not shown).

After 48 h incubation of AOH (50 μM in medium), the total recovery of the applied amount as extractable conjugates was only about 50%, and the major proportion (80%) of the recovered material consisted of the monoglucosides 9-*O*-*β*-D-glucopyranosyl-AOH (60%) and 3-*O*-*β*-D-glucopyranosyl-AOH (20%). Notably, the corresponding malonylated 9-*O*- and 3-*O*-glucosides of AOH together accounted for only 13% of the extractable conjugates. This pattern did not differ much at incubation times of 24 and 96 h. The major difference was an increase of 9-*O*-{*β*-D-glucopyranosyl(1 → 6)-*β*-D-glucopyranosyl}AOH from 7% at 24 h to 25% at 96 h, accompanied by a decrease of 9-*O*-*β*-D-glucopyranosyl-AOH (data not shown). In addition, the total recovery of extractable AOH metabolites decreased to about 35%.

Implications. Our study demonstrated that the *Alternaria* toxins AOH and AME are efficiently conjugated in cultured tobacco BY-2 cells, a widely used *in vitro* model for plant cell metabolism. The first metabolic step for both mycotoxins is conjugation with glucose. Metabolic conjugation during phase II metabolism is comparable in mammals and plants and considered an important first detoxification step for endogenous and exogenous compounds.[22] Major differences, however, between mammals and plants exist in the fate of such conjugated metabolites. Whereas animals and humans are able to rapidly excrete phase II metabolites via urine and bile, plants are basically unable to excrete phase II metabolites. Thus, storage of the metabolites either as soluble conjugates in vacuoles or as insoluble conjugates bound to cell wall components becomes essential. Both options require further modification of the primary conjugates. Whereas malonylation of the glucoside is considered a signal for transport into vacuoles, further glycosylation is supposed to enable incorporation into the cell wall.[22] Both processes are, however, not well understood on a molecular and cellular level. From our first semiquantitative data it appears that malonyl conjugation of the primarily formed glucosides is the preferred pathway for AME, whereas AOH is glycosylated, but less readily malonylated. Thus, it can be assumed that AME detoxification through conjugation and storage in the vacuole is a more efficient process for AME as compared to AOH. The efficient formation of malonyl glucosides and their potential storage in the vacuole may also explain the comparatively high recoveries for AME in our experiments, whereas much less AOH was recovered. Thus, it can be assumed that AOH is preferentially stored in the cell wall, a hypothesis that, however, needs to be investigated in future studies.

Another difference observed between AOH and AME incubations was related to cell growth. Growth of cells

DOI: 10.1021/acs.jafc.5b00806
J. Agric. Food Chem. 2015, 63, 4728−4736

incubated with AME was comparable to control cells without mycotoxin; a reduction of cell mass was, however, noted if the cells were incubated with AOH. Therefore, cell cultures were treated during the lag phase of growth with the mycotoxins (50 μM in medium) for 24, 48, and 72 h, and the wet weight of cells was determined. An aliquot of the cells was stained with Evans blue to indicate dead cells and scored by light microscopy. Whereas the cell mass of AME-treated cells increased up to 6 fold with a slight decrease of dead cells, no significant increase in the cell mass was observed in AOH-treated cells, but the percentage of dead cells increased up to 40% over time. Thus, the impact of *Alternaria* toxins and their conjugates on phytotoxicity is another factor that needs to be investigated in future studies.

While we unambiguously proved the formation of conjugates of *Alternaria* toxins in cell suspensions, the formation of these conjugates also needs to be demonstrated in field plants as a first step to evaluate a potential impact of AOH and AME conjugates on food and feed safety. A very first approach to measure conjugated *Alternaria* toxins was performed by Walravens and co-workers who developed an UPLC-MS/MS method to analyze glucosylated AOH and AME using synthesized standard compounds.[23] Syntheses of 9-*O*-β-D-glucopyranosyl-AOH, 3-*O*-β-D-glucopyranosyl-AOH, and 3-*O*-β-D-glucopyranosyl-AME were described by Mikula et al.,[24] but only 3-*O*-β-D-glucopyranosyl-AOH and 3-*O*-β-D-glucopyranosyl-AME were used for the method development mentioned above. Analyses of 24 cereal-based food products did not detect any 3-*O*-β-D-glucopyranosyl-AOH (the less abundant glucose-conjugated AOH metabolite in our study) or 3-*O*-β-D-glucopyranosyl-AME in these samples, which, however, did not contain AME, too, and only trace amounts of AOH. Therefore, more studies that include the full array of metabolites identified in our study using food products from different plant families are required to estimate the impact of AOH and AME conjugates on food and feed safety.

■ ASSOCIATED CONTENT

Supporting Information

HSQC and HMBC spectra of all AOH and AME metabolites identified in this study. The Supporting Information is available free of charge on the ACS Publications website at DOI: 10.1021/acs.jafc.5b00806.

■ AUTHOR INFORMATION

Corresponding Author

*Tel: +4972160842936. E-mail: mirko.bunzel@kit.edu.

Notes

The authors declare no competing financial interest.

■ ACKNOWLEDGMENTS

The authors are grateful to Dr. Jan Maisch (Institute of Botany, KIT) for providing BY-2 cells.

■ ABBREVIATIONS

AME, alternariol-9-*O*-monomethyl ether; AOH, alternariol; HPAEC, high performance anion exchange chromatography; PAD, pulsed amperometric detection; PDA, photo diode array; UGT, UDP-glucuronosyl transferase

■ REFERENCES

(1) Logrieco, A.; Moretti, A.; Solfrizzo, M. Alternaria toxins and plant diseases: An overview of origin, occurrence and risks. *World Mycotoxin J.* **2009**, *2*, 129−140.

(2) Ostry, V. Alternaria mycotoxins: An overview of chemical characterization, producers, toxicity, analysis and occurrence in foodstuffs. *World Mycotoxin J.* **2008**, *1*, 175−188.

(3) Liu, G. T.; Qian, Y. Z.; Zhang, P.; Dong, W. H.; Qi, Y. M.; Guo, H. T. Etiological role of Alternaria alternata in human esophageal cancer. *Chin. Med. J. (Engl)* **1992**, *105*, 394−400.

(4) EFSA. Scientific opinion on the risks for animal and public health related to the presence of *Alternaria* toxins in feed and food. *EFSA J.* **2011**, *9* (2407), 97.

(5) Lehmann, L.; Wagner, J.; Metzler, M. Estrogenic and clastogenic potential of the mycotoxin alternariol in cultured mammalian cells. *Food Chem. Toxicol.* **2006**, *44*, 398−408.

(6) Brugger, E. M.; Wagner, J.; Schumacher, D. M.; Koch, K.; Podlech, J.; Metzler, M.; Lehmann, L. Mutagenicity of the mycotoxin alternariol in cultured mammalian cells. *Toxicol. Lett.* **2006**, *164*, 221−230.

(7) Pfeiffer, E.; Eschbach, S.; Metzler, M. *Alternaria* toxins: DNA strand-breaking activity in mammalian cells in vitro. *Mycotoxin Res.* **2007**, *23*, 152−157.

(8) Fehr, M.; Pahlke, G.; Fritz, J.; Christensen, M. O.; Boege, F.; Altemoller, M.; Podlech, J.; Marko, D. Alternariol acts as a topoisomerase poison, preferentially affecting the IIalpha isoform. *Mol. Nutr. Food Res.* **2009**, *53*, 441−451.

(9) Pfeiffer, E.; Schmit, C.; Burkhardt, B.; Altemöller, M.; Podlech, J.; Metzler, M. Glucuronidation of the mycotoxins alternariol and alternariol-9-methyl ether in vitro: Chemical structures of glucuronides and activities of human UDP-glucuronosyltransferase isoforms. *Mycotoxin Res.* **2009**, *25*, 3−10.

(10) Sandermann, H. Plant metabolism of xenobiotics. *Trends Biochem. Sci.* **1992**, *17*, 82−84.

(11) Gareis, M.; Bauer, J.; Thiem, J.; Plank, G.; Grabley, S.; Gedek, B. Cleavage of zearalenone-glycoside, a masked mycotoxin, during digestion in swine. *J. Vet. Med. B* **1990**, *37*, 236−240.

(12) Berthiller, F.; Crews, C.; Dall'Asta, C.; De Saeger, S.; Haesaert, G.; Karlovsky, P.; Oswald, I. P.; Seefelder, W.; Speijers, G.; Stroka, J. Masked mycotoxins: A review. *Mol. Nutr. Food Res.* **2013**, *57*, 165−186.

(13) EFSA. Scientific opinion on the risks for human and animal health related to the presence of modified forms of certain mycotoxins in food and feed. *EFSA J.* **2014**, *12* (3916), 107.

(14) Rychlik, M.; Humpf, H. U.; Marko, D.; Danicke, S.; Mally, A.; Berthiller, F.; Klaffke, H.; Lorenz, N. Proposal of a comprehensive definition of modified and other forms of mycotoxins including "masked" mycotoxins. *Mycotoxin. Res.* **2014**, *30*, 197−205.

(15) Fleck, S. C.; Burkhardt, B.; Pfeiffer, E.; Metzler, M. Alternaria toxins: Altertoxin II is a much stronger mutagen and DNA strand breaking mycotoxin than alternariol and its methyl ether in cultured mammalian cells. *Toxicol. Lett.* **2012**, *214*, 27−32.

(16) Turner, J. G.; Novacky, A. Quantitative relation between plant and bacterial cells involved in hypersensitive reaction. *Phytopathology* **1974**, *64*, 885−890.

(17) Wefers, D.; Tyl, C. E.; Bunzel, M. Novel arabinan and galactan oligosaccharides from dicotyledonous plants. *Front. Chem.* **2014**, *2*, 100.

(18) Gottlieb, H. E.; Kotlyar, V.; Nudelman, A. NMR chemical shifts of common laboratory solvents as trace impurities. *J. Org. Chem.* **1997**, *62*, 7512−7515.

(19) Yerramsetty, V.; Mathias, K.; Bunzel, M.; Ismail, B. Detection and structural characterization of thermally generated isoflavone malonylglucoside derivatives. *J. Agric. Food. Chem.* **2011**, *59*, 174−83.

(20) Kovalsky Paris, M. P.; Schweiger, W.; Hametner, C.; Stuckler, R.; Muehlbauer, G. J.; Varga, E.; Krska, R.; Berthiller, F.; Adam, G. Zearalenone-16-*O*-glucoside: a new masked mycotoxin. *J. Agric. Food. Chem.* **2014**, *62*, 1181−1189.

DOI: 10.1021/acs.jafc.5b00806
J. Agric. Food Chem. 2015, 63, 4728−4736

(21) Yoshimoto, K.; Tsuda, Y. General path of *O*-acyl migration in D-glucose derivatives: acyl migration of methyl mono-*O*-myristoyl-*α*- and *β*-D-glucopyranosides and mono-O-myristoyl-D-glucopyranoses. *Chem. Pharm. Bull.* **1983**, *31*, 4324−34.
(22) Sandermann, H. Higher-plant metabolism of xenobiotics-the green liver concept. *Pharmacogenetics* **1994**, *4*, 225−241.
(23) Walravens, J.; Mikula, H.; Rychlik, M.; Asam, S.; Ediage, E. N.; Di Mavungu, J. D.; Van Landschoot, A.; Vanhaecke, L.; De Saeger, S. Development and validation of an ultra-high-performance liquid chromatography tandem mass spectrometric method for the simultaneous determination of free and conjugated Alternaria toxins in cereal-based foodstuffs. *J. Chromatogr. A* **2014**, *1372*, 91−101.
(24) Mikula, H.; Skrinjar, P.; Sohr, B.; Ellmer, D.; Hametner, C.; Froehlich, J. Total synthesis of masked Alternaria mycotoxins-sulfates and glucosides of alternariol (AOH) and alternariol-9-methyl ether (AME). *Tetrahedron* **2013**, *69*, 10322−10330.

DOI: 10.1021/acs.jafc.5b00806
J. Agric. Food Chem. 2015, 63, 4728−4736